Photochemistry and Photobiology, 2022, 98: 57–61

Special Issue Research Article

Estimation of Singlet Oxygen Quantum Yield Using Novel Green-Absorbing Baird-type Aromatic Photosensitizers†

Jayla Morgan[1‡], Young Ju Yun[1,2‡] and A. Jean-Luc Ayitou PhD[1,2*]

[1]Department of Chemistry, Illinois Institute of Technology, Chicago, IL,
[2]Department of Chemistry, University of Illinois at Chicago, Chicago, IL,

Received 16 February 2021, revised 30 May 2021, accepted 4 July 2021, DOI: 10.1111/php.13483

ABSTRACT

We report two new organic green-absorbing singlet oxygen ($^1O_2$) photosensitizers: Quinoidal naphthyl thioamide (QDM) and *bis*-iodol-dipyrrolonaphthyridine-dione (I_2–DPND), with triplet energies of 40.8 and 47.5 kcal mol^{-1}(at 77 K in a glassy matrix) , respectively. The UV–vis absorption and emission characteristics of QDM and I_2–DPND are similar to other commercially available organic $^1O_2$ photosensitizers such as Rose Bengal, which was used as standard/reference to estimate the $^1O_2$ quantum yield (Φ_Δ) of the chromophores under study. Using 9,10-diphenylanthracene (DPA) as an $^1O_2$ quencher, we estimated the $\Phi_\Delta \approx$ 67–85% for QDM and $\Phi_\Delta \approx$ 25–32% for I_2–DPND. The discrepancy in the Φ_Δ values could be explained by the apparent photodecomposition of the later dye. Nevertheless, the high Φ_Δ value for QDM is unprecedented, as this chromophore exhibits relatively low structural complexity and could further be derivatized to create novel photodynamic agents.

INTRODUCTION

In recent years, photodynamic therapy (PDT) has been demonstrated to be a powerful technique, yet less-aggressive, biomedical approach to treat a number of malignant tumors (1,2). Fundamentally, the PDT technique relies on the absorption of visible-to-NIR light energy by a dye or photosensitizer molecule (PS), which upon excitation, undergoes energy exchange with molecular oxygen ($^3O_2$) to generate a reactive oxygen species (ROS) (3) via either the type I ($O_2^{-\bullet}$, H_2O_2, ·OH) or type II ($^1O_2$) mechanism (4). It is a general consensus that the efficacy of PDT depends on the lifetime of the ROS (5), specifically $^1O_2$; but, the other most important factor is the lifetime of the excited PS (PS*) (3). Up to date, the reported PS molecules exhibit, not only various degrees of structural complexity, but also excited state behavior/lifetime that would dictate the outcome of the bimolecular process to generate the ROS and the efficacy of the PDT. For example, Photofrin II (6,7), the first approved PS by the FDA in the 1990s to treat esophageal and early stage of lung cancer, is a complex mixture of oligomers of porphyrin. Photofrin II is known to have long-lasting photodynamic effects due to the large amount (2–10 mg/kg of body weight) required for effective treatment of the malignant tumors (7). Importantly, in recent years, many other PS have been developed/reported (8,9) to be more or less effective than Photofrin II. The excited state behaviors of reported PS are based on (or dictated by) classical photophysical paradigms *viz*. spin-orbit coupling and heavy-atom effect (10) that allow modulation of the photo-excitation of the PS molecule(s) and the lifetime/behavior of PS*. To the best of our knowledge, no reported PS molecule has been shown to exhibit Baird aromaticity (11) in their excited state, whereby the photo-behavior of the PS/PS* is entirely governed by a reversal (or enhancement) of aromaticity allowing a better stabilization of the (triplet) excited state of the PS molecule. Herein, we report two new purely organic chromophores (Scheme 1): quinoidal naphthyl thioamide (**QDM**) ($E_T \approx$ 40.8 kcal mol^{-1}, in 77 K EtOH:DCM glassy matrix) and *bis*-iodol-dipyrrolonaphthyridine-dione (**I_2–DPND**) ($E_T \approx$ 47.5 kcal mol^{-1}, in 77 K EtOH:DCM glassy matrix) which could be used as potential PS scaffolds to develop novel biorelevant photodynamic agents.

According to the Baird rule of aromaticity, conjugated 4nπ annulenes that exhibit ground state antiaromaticity would be able to populate their lowest T_1 state due to aromaticity reversal (11–13). Hence, chromophores that exhibit Baird-type aromaticity are scarce, since the ground state structure(s) of these systems would be antiaromatic. However, there have been synthetic efforts to create nonclassical polyaromatic chromophores with individual rings exhibiting either paratropic or diatropic ring current (14). Accordingly, Baird-type chromophores are globally aromatic, but at least one ring (with a π-conjugation) within these systems would be anti/non/proaromatic or exhibit paratropic ring current (15). When this condition is met, it is believed that the chromophore of interest would be able to access its triplet state following the Baird rule.

We had previously employed **QDM** as a Baird-type heavy-atom-free aromatic triplet chromophore to sensitize polyaromatic hydrocarbons and achieved triplet–triplet annihilation based photon upconversion (TTA-UC) (16–18). Dipyrrolonaphthyridine-dione (**DPND**), the precursor of **I_2–DPND,** was first reported by Gryko and Kozankiewicz (19) and later utilized by Wang,

*Corresponding author email: aayitou@iit.edu (A. Jean-Luc Ayitou)
†This article is part of a Special Issue dedicated to the memory of Dr. Karen Brewer.
‡These authors have contributed equally to this work.

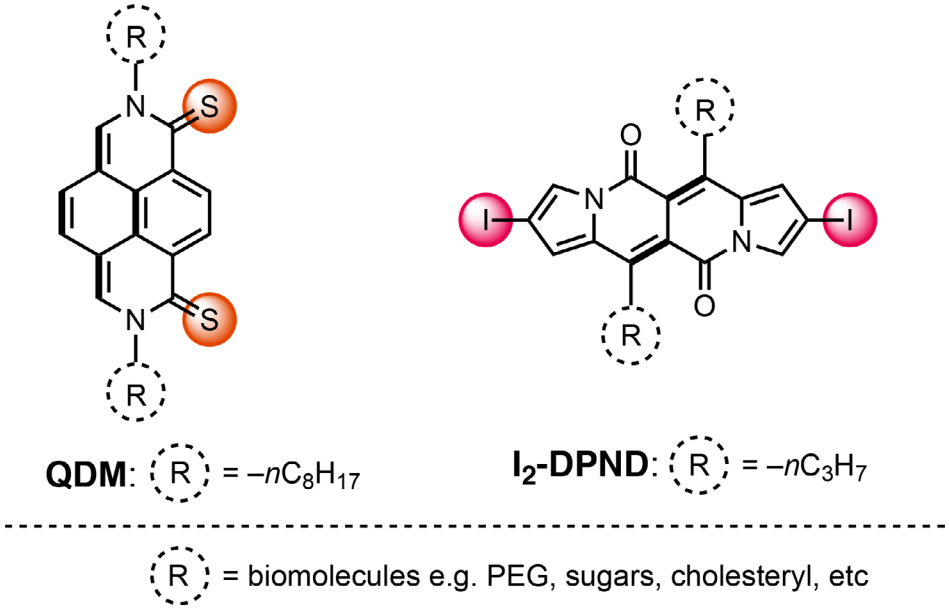

Scheme 1. Chemical structures of novel PDT dye **QDM** and **I_2–DPND**. Also shown are the possible modification sites with biomolecules.

Zhu and Fu to achieve singlet fission (SF) in the solid state (20). Even though **DPND** emits strongly in solution at room temperature ($\Phi_F \approx 70\%$), Fu et al. demonstrated that this dye can achieve efficient intersystem crossing (ISC) in the solid state via SF thanks to an increase in aromaticity character (or aromaticity reversal) in the lowest T_1 state (20). Armed with the promising report on the photophysics of **DPND**, we used iodination (heavy-atom) technique to enhance ISC within **DPND**. In the present report, we show that both **QDM** and **I_2–DPND** can be employed as $^1O_2$ PS, and their relatively simple structural features may be useful in achieving facile derivatizations to create other organic or biorelevant photodynamic agents.

MATERIALS AND METHODS

Experimental section. The synthetic procedures leading to **QDM** and **I_2–DPND** are thoroughly described in the Supporting Information (Scheme S1). **QDM** and **I_2–DPND** and their corresponding precursors have been fully characterized by NMR spectroscopy. All commercially obtained reagents/solvents were used as received without further purification. UV–vis absorption spectra were recorded on an Ocean Optics® spectrometer (DH-MINI UVVIS-NIR Light Source and QE–Pro detector using Oceanview® software package). Emission spectra were recorded on an Edinburgh Instrument FLS980 spectrometer. Spectroscopy grade dichloromethane (DCM) and ethanol (EtOH) solvents were used for all photophysical measurements.

Singlet oxygen quantum yield (Φ_Δ) measurement. Since both **QDM** and **I_2–DPND** absorb in the green-to-yellow spectral region, singlet oxygen sensitization/generation studies were performed using a commercial 532 ± 5 nm (green) laser of 50 mW cm^{-2} power density. 9,10-diphenyl anthracene (**DPA**) was used as the $^1O_2$ quencher (Scheme 2) (21). Samples of sensitizers and **DPA** were O_2 saturated for at least 30 minutes prior to irradiation. The spectral change/reduction in the absorbance/O.D. of the DCM:EtOH (1:1, v/v) of **DPA** at 393 nm (due to the [4 + 2] cycloaddition reaction with $^1O_2$) was monitored over 15 min at various time intervals (20 s, 40 s, 60 s, 80 s, 100 s, 120 s, 240 s, 360 s, 480 s, 600 s and 900 s). The relative quantum yield (Φ_Δ) was measured against the value of Rose Bengal which was used as reference/standard. Φ_Δ values were estimated using the following equation (Eq. 1) (22,23).

$$\Phi_{\Delta,\text{sample}} = \Phi_{\Delta,\text{ref}} * \left(\frac{F_{\text{ref}}}{F_{\text{sample}}}\right) * \left(\frac{m_{\text{sample}}}{m_{\text{ref}}}\right) * \left(\frac{\eta_{\text{sample}}}{\eta_{\text{ref}}}\right)^2 \quad (1)$$

Where ref denotes the reference/standard (Rose Bengal: $\Phi_\Delta = 0.68$ (24) and $\Phi_\Delta = 0.86$ (25–28) in EtOH); F is the absorption correction factor, which can be calculated from the formula.

$F = 1–10^{-OD}$ (with O.D. at the excitation wavelength 532 nm); m represents the slope of the absorbance of **DPA** (393 nm) with given excitation time, and η symbolizes the refractive index of the solvent used for measurement (η for DCM = 1.424 and η for EtOH = 1.362).

RESULTS AND DISCUSSION

UV–vis absorption and emission spectra

As depicted in Fig. 1, **QDM** and **I_2–DPND** can harvest green-to-yellow photons up to 580 nm with maximum absorption at ca. 450 nm. It is worth noting that the absorption maximum for **I_2–DPND** was red-shifted with increase in degree of iodination of parent **DPND** core (see Supporting Information, Figure S7). The steady state $S_0 \longleftarrow S_1$ emission bands with $\lambda_{max} \approx 545$ nm (for **QDM**) and 582 nm (for **I_2–DPND**) produced quantum yield (Φ_F) of 0.2% and 2.5%, respectively. With these lower values for the Φ_F, it will be justified to investigate ISC or record the $S_0 \longleftarrow T_1$ emissions as well. The phosphorescence emissions for the two chromophores were successfully recorded in DCM:EtOH (1:1, v/v) glass at 77 K with $\lambda_{max} \approx 725$ ($\tau_{Phos} = 0.4$ ms) for **QDM** and 680 nm ($\tau_{Phos} = 14.8$ ms) for **I_2–DPND**.

Singlet oxygen studies

The singlet oxygen ($^1O_2$) generation ability of **QDM** and **I_2–DPND** was investigated using the absorption/chemical method, where the decrease in absorption of **DPA** in the irradiated oxygenated samples of these sensitizers is indicative of depletion or photo-oxidation of **DPA** molecules. It is well documented that $^1O_2$ reacts with alkenes or π-conjugated scaffolds via the ene- or [4 + 2] cycloaddition reactions to produce peroxides (25). In the

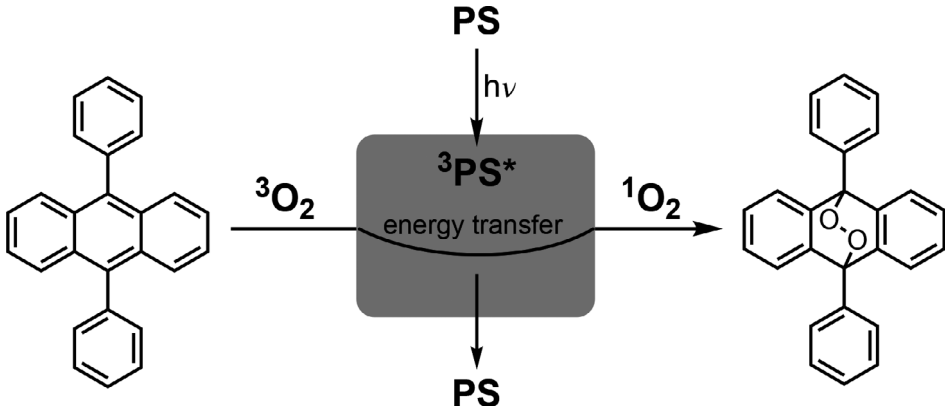

Scheme 2. Photo-oxygenation of **DPA** in oxygen saturated solutions of PS (**QDM** and/or **I$_2$–DPND**).

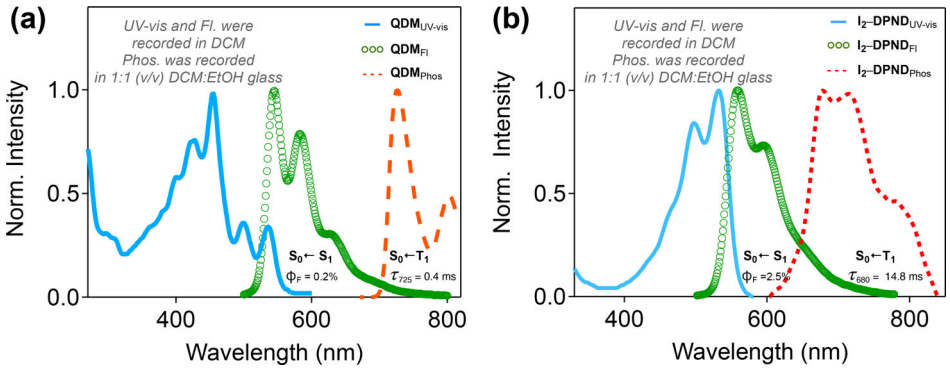

Figure 1. UV–vis absorption and emission profiles of (a) **QDM** and (b) **I$_2$–DPND**: The emission spectra were obtained with samples with samples of O.D. = 0.2 at the excitation wavelength.

present work, the photo-oxidation of **DPA** (22) was monitored over 15 min, at what time we assumed complete depletion of dissolved molecular oxygen in the solutions. The changes in the absorption band of **DPA** at 393 nm are illustrated in Fig. 2a–c. Rose Bengal was employed as reference/standard with two different reported singlet oxygen Φ_Δ values: $\Phi_\Delta = 0.68$ (25) and $\Phi_\Delta = 0.86$ (29) in EtOH. Using Eq. 1, the Φ_Δ for **QDM** was estimated at 0.67 (with $\Phi_{\Delta,RB} = 0.68$) and 0.85 (with $\Phi_{\Delta,RB} = 0.86$) and that of **I$_2$–DPND** was 0.25 (with $\Phi_{\Delta,RB} = 0.68$) and 0.32 (with $\Phi_{\Delta,RB} = 0.86$) (Table 1). It is worth noting that over the course of the experiment, while **QDM** seemed photo-stable just like the reference Rose Bengal, the absorption band of **I$_2$–DPND** between 430 and 580 nm gradual decreased and a new band appeared between 330 nm and 430 nm. This change/variation in absorption is suggestive of photo-bleach or conversion to a new species, which we hypothesize to be a deiodinated by-product (such as **I–DPND** or **DPND**). Apparently, the change in absorption was more pronounced in DCM than in DCM:EtOH (1:1, v/v) (Figure S8) with 20% of the absorption of **I$_2$–DPND** decreased in DCM within 120 s compared to 6% in DCM:EtOH (1:1, v/v) within the same timeframe. Moreover, the degradation of **I$_2$–DPND** upon photo-irradiation seemed to be amplified in oxygen saturated samples than in N_2 purged samples (see Supporting Information, Figure S9). While 43% of **I$_2$–DPND** degraded after 900 s in the oxygen saturated samples, only 25% of the chromophore was decomposed in the N_2 purged samples. Even when a trace amount of oleic acid (as a scavenger for singlet oxygen) was added to a sample of **I$_2$–DPND**, 30% of **I$_2$–DPND** decomposed over 900 s of irradiation (see Supporting Information, Figure S10b). Although these mixed results were not conclusive to the actual causes of the apparent photo-decomposition of **I$_2$–DPND**, we suggest that the C–I bond could be undergoing scission during the irradiation, and no photo-oxidation was occurring as evidenced by the variation in the whole absorption band. Subsequently, the apparent photo-induced loss of iodine of **I$_2$–DPND** was further investigated by ^{1}H NMR, as shown in Figure S11, the irradiation of a concentrated solution of this chromophore using a medium pressure Hg lamp (450 W) with a 500 nm cutoff revealed the appearance of NMR patterns of parent **DPND** after 4 h of irradiation time (see Supporting Information, Figure S3). This result suggests a likely deiodination of **I$_2$–DPND**; and it is in agreement with the low value of Φ_Δ for **I$_2$–DPND**, as the photo-decomposition is likely competing with the energy transfer to $^3O_2$.

In summary, we report the synthesis and photophysical characterization of two new organic photosensitizers **QDM** and **I$_2$–DPND**, whose photophysical trajectories are governed by the Baird rule. From the UV–vis absorption and emission studies, we showed that **QDM** and **I$_2$–DPND** could absorb light in the biological window and generate ROS ($^1O_2$) via the type II photosensitization mechanism (30,31). Using **DPA** as $^1O_2$ quencher and Rose Bengal as standard/reference, we estimated the quantum yield (Φ_Δ) of $^1O_2$ production as high as 85% for **QDM** and only 32% for **I$_2$–DPND**. We propose that the low value of the

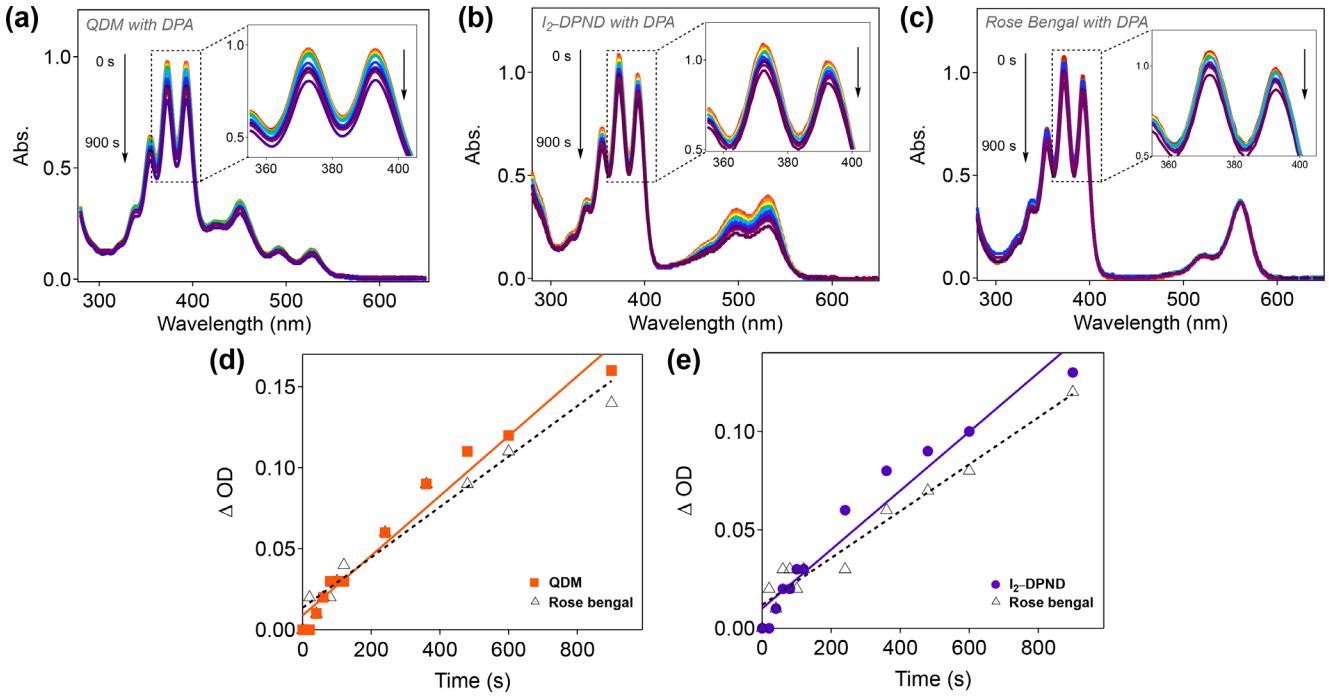

Figure 2. Changes in the absorption spectrum of **DPA** (photo-oxidation) upon irradiation using a 532 nm laser in the presence of (a) **QDM**, (b) **I_2–DPND**, (c) **Rose Bengal** and (d and e) linear changes in absorbance of **DPA** at 393 nm as function of irradiation time in O_2 saturated solutions of DCM:EtOH (1:1, v/v): The O.D. at λ_{532} for all three samples was 0.4; Rose Bengal was used as reference for both **QDM** and **I_2–DPND**.

Table 1. Photophysical parameters of **QDM** and **I_2–DPND**.

	λ_{abs}*	λ_{FL}*	Φ_F (%)*	λ_{Phos}†	τ_{Phos} §	E_{S1} (kcal/mol)	E_{T1} (kcal/mol)	Φ_Δ (%)¶
QDM	454 nm	544 nm	0.2‡	725 nm	0.4 ms	50	40.8	67** (85††)
I_2–DPND	532 nm	559 nm	2.5‡	678 nm	14.8 ms	52.4	47.5	25** (32††)

*Recorded in DCM for **QDM** and **I_2–DPND**; †Recorded in DCM:EtOH (1:1, v/v) glass at 77K; ‡Relative value for **QDM** and absolute value for **I_2–DPND** recorded in DCM ; §Monitored at 725 nm for **QDM** and 680 nm for **I_2–DPND**; ¶Singlet oxygen quantum yields using samples of **QDM** and **I_2–DPND** (with O.D. = 0.4 at λ_{532}) in the presence of quencher **DPA** (O.D. = 1.0 at λ_{532}). Rose Bengal was used as standard with reported singlet oxygen quantum yield; **Φ_Δ = 0.68 (25); ††Φ_Δ = 0.86 (29) in EtOH.

Φ_Δ for **I_2–DPND** was likely due to a competing photodecomposition of this chromophore as evidenced in the variation of its absorption. Nevertheless, the present report highlights the possibility to create new organic Baird-type aromatic PS which can be further derivatized to create other biorelevant photodynamic agents.

Acknowledgements—This work was supported in part by the National Science Foundation under a CAREER grant no. 1753012 Awarded to AJA and Illinois Tech Graduate Kilpatrick and Starr Fieldhouse Fellowships to YJY.

SUPPORTING INFORMATION

Additional supporting information may be found online in the Supporting Information section at the end of the article:

Chart S1. Chemical structures of **QDM, I2–DPND** and their precursors.

Scheme S1. Syntheses of (a) **QDM** and (b) **I2–DPND**.

Scheme S2. Synthetic route for **QDM**.

Scheme S3. Synthetic route for **Dipyrrole**.

Scheme S4. Synthetic route for **DPND**.

Scheme S5. Synthetic route for **I2–DPND**.

Figure S1. ^{1}H NMR spectrum (300 MHz) of **Dipyrrole** in CDCl3. *Residual solvent peak of CHCl3.

Figure S2. ^{13}C NMR spectrum (75 MHz) of **Dipyrrole** in CDCl3. *Residual solvent peak of CHCl3.

Figure S3. ^{1}H NMR spectrum (300 MHz) of **DPND** in CDCl3. *Residual solvent peak of CHCl3.

Figure S4. ^{13}C NMR spectrum (75 MHz) of **DPND** in CDCl3. *Residual solvent peak of CHCl3.

Figure S5. ^{1}H NMR spectrum (300 MHz) of **I2–DPND** in CDCl3. *Residual solvent peak of CHCl3.

Figure S6. ^{13}C NMR spectrum (75 MHz) of **I2–DPND** in CDCl3. *Residual solvent peak of CHCl3.

Figure S7. UV–vis and emission profiles of **DPND** and **I2–DPND** in DCM with O.D. = 0.2.

Figure S8. Changes in the absorption spectrum of **I2–DPND** upon 532 nm irradiation (a) in DCM and (b) in DCM : EtOH (1:1, v/v).

Figure S9. Changes in the absorption spectrum of **I2–DPND** upon 532 nm irradiation in DCM : EtOH (1:1, v/v). (a)

anaerobic condition under N2 atmosphere (b) in the presence of singlet oxygen scavenger (trace amount of oleic acid).

Figure S10. Changes in the absorption spectrum of **I2–DPND** upon 532 nm irradiation (a) in O2 saturated DCM : EtOH (1:1, v/v) and (b) in N2 saturated DCM : EtOH (1:1, v/v).

Figure S11. Time-course investigation of the photo-decomposition of **I2–DPND** upon irradiation in an NMR tube (concentrated solution) using a medium pressure Hg lamp (450 W) using a 500 nm cutoff: The expanded area of this set of spectra shows the appearance of NMR patterns of parent DPND (cf. Figure S3) suggesting a likely deiodination of **I2–DPND**.

REFERENCES

1. Dougherty T. J. (2002) An Update on Photodynamic Therapy Applications. *Journal of Clinical Laser Medicine & Surgery*. **20**(1), 3–7. http://dx.doi.org/10.1089/104454702753474931
2. Dougherty, T. J. and S. L. Marcus (1992) Photodynamic therapy. *Eur. J. Cancer* **28**, 1734–1742.
3. Takemura, T., N. Ohta, S. Nakajima and I. Sakata (1989) Critical importance of the triplet lifetime of photosensitizer in photodynamic therapy of tumor. *Photochem Photobiol.* **50**(3), 339–344.
4. Wilson, B. C. and M. S. Patterson (2008) The physics, biophysics and technology of photodynamic therapy. *Phys. Med. Biol.* **53**, R61–R109.
5. Ormond, A. and H. Freeman (2013) Dye sensitizers for photodynamic therapy. *Materials.* **6**, 817–840.
6. He, X. Y., R. A. Sikes, S. Thomsen, L. W. K. Chung and S. L. Jacques (1994) Photodynamic therapy with photofrin II induces programmed cell death in carcinoma cell lines. *Photochem Photobiol.* **59**(4), 468–473.
7. Nowak-Sliwinska, P., A. Karocki, M. Elas, A. Pawlak, G. Stochel and K. Urbanska (2006) Verteporfin, photofrin II, and merocyanine 540 as PDT photosensitizers against melanoma cells. *Biochem. Biophys. Res.* **349**, 549–555.
8. McKenzie L. K., H. E. Bryant, J. A. Weinstein (2019) Transition metal complexes as photosensitisers in one- and two-photon photodynamic therapy. *Coordination Chemistry Reviews*. **379**, 2–29. http://dx.doi.org/10.1016/j.ccr.2018.03.020
9. Zhou, Z., J. Song, L. Nie and X. Chen (2016) Reactive oxygen species generating systems meeting challenges of photodynamic cancer therapy. *Chem Soc Rev.* **45**, 6597–6626.
10. Padilla R., W. A. Maza, A. J. Dominijanni, B. S. J. Winkel, A. J. Morris, K. J. Brewer (2016) Pushing the limits of structurally-diverse light-harvesting Ru(II) metal-organic chromophores for photodynamic therapy. *Journal of Photochemistry and Photobiology A: Chemistry*. **322-323**, 67–75. http://dx.doi.org/10.1016/j.jphotochem.2016.02.006
11. Baird N. C. (1972) Quantum organic photochemistry. II. Resonance and aromaticity in the lowest 3.pi..pi.* state of cyclic hydrocarbons. *Journal of the American Chemical Society*. **94**: 14, 4941–4948. http://dx.doi.org/10.1021/ja00769a025
12. Rosenberg, M., C. Dahlstrand, K. Kilså and H. Ottosson (2014) Excited state aromaticity and antiaromaticity: opportunities for photophysical and photochemical rationalizations. *Chem. Rev.* **114**(10), 5379–5425.
13. Ottosson H. (2012) Exciting excited-state aromaticity. *Nature Chemistry*. **4**(12), 969–971. http://dx.doi.org/10.1038/nchem.1518
14. Wiberg, K. B. (2001) Antiaromaticity in monocyclic conjugated carbon rings. *Chem. Rev.* **101**(5), 1317–1331.
15. Escayola, S., C. Tonnelé, E. Matito, A. Poater, H. Ottosson, M. Solà and D. Casanova (2021) Guidelines for tuning the excited state Hückel-Baird hybrid aromatic character of pro-aromatic quinoidal compounds. *Angew. Chem. Int. Ed.* **60**(18), 10255–10265.
16. Shokri S., G. P. Wiederrecht, D. J. Gosztola, A. J. -L. Ayitou (2017) Photon Upconversion Using Baird-Type (Anti)Aromatic Quinoidal Naphthalene Derivative as a Sensitizer. *The Journal of Physical Chemistry C*. **121**(42), 23377–23382. http://dx.doi.org/10.1021/acs.jpcc.7b08373
17. Yun Y. J., N. Kamatham, M. K. Manna, J. Li, S. Liu, G. P. Wiederrecht, D. J. Gosztola, B. T. Diroll, A. Y. Rogachev, A. J. -L. Ayitou (2020) Interplay between Energy and Charge Transfers in a Polyaromatic Triplet Donor–Acceptor Dyad. *The Journal of Physical Chemistry C*. **124**(23), 12205–12212. http://dx.doi.org/10.1021/acs.jpcc.0c01530
18. Shokri, S., J. Li, M. K. Manna, G. P. Wiederrecht, D. J. Gosztola, A. Ugrinov, S. Jockusch, A. Yu Rogachev and A.-J.-L. Ayitou (2017) A Naphtho- p-quinodimethane exhibiting Baird's (anti)aromaticity, broken symmetry, and attractive photoluminescence. *J. Org. Chem.* **82**, 10167–10173.
19. Grzybowski, M., I. Deperasińska, M. Chotkowski, M. Banasiewicz, A. Makarewicz, B. Kozankiewicz and D. T. Gryko (2016) Dipyrrolonaphthyridinediones – structurally unique cross-conjugated dyes. *Chem. Commun.* **52**, 5108–5111.
20. Wang, L., L. Lin, J. Yang, Y. Wu, H. Wang, J. Zhu, J. Yao and H. Fu (2020) Singlet fission in a pyrrole-fused cross-conjugated skeleton with adaptive aromaticity. *J. Am. Chem. Soc.* **142**, 10235–10239.
21. Swart, M. (2020) Bond orders in metalloporphyrins. *Theor. Chem. Acc.* **139**, 1–8.
22. Steinbeck, M. J., A. U. Khan and M. J. Karnovsky (1992) Intracellular singlet oxygen generation by phagocytosing neutrophils in response to particles coated with a chemical trap. *J. Biol. Chem.* **267**, 13425–13433.
23. Imran M., A. M. El-Zohry, C. Matt, M. Taddei, S. Doria, L. Bussotti, P. Foggi, J. Zhao, M. Di Donato, O. F. Mohammed, S. Weber (2020) Intersystem crossing via charge recombination in a perylene–naphthalimide compact electron donor/acceptor dyad. *Journal of Materials Chemistry C*. **8**(24), 8305–8319. http://dx.doi.org/10.1039/d0tc00017e
24. Adarsh, N., R. R. Avirah and D. Ramaiah (2010) Tuning photosensitized singlet oxygen generation efficiency of novel Aza-BODIPY dyes. *Org. Lett.* **12**, 5720–5723.
25. DeRosa, M. C. and R. J. Crutchley (2002) Photosensitized singlet oxygen and its applications. *Coord. Chem. Rev.* **233–234**, 351–371.
26. Mathai, S., T. A. Smith and K. P. Ghiggino (2007) Singlet oxygen quantum yields of potential porphyrin-based photosensitisers for photodynamic therapy. *Photochem. Photobiol. Sci.* **6**, 995–1002.
27. Xiao, L., L. Gu, S. B. Howell and M. J. Sailor (2011) Porous silicon nanoparticle photosensitizers for singlet oxygen and their phototoxicity against cancer cells. *ACS Nano* **5**, 3651–3659.
28. Hoebeke, M., A. Seret, J. Piette and A. Van de Vorst (1988) Singlet oxygen production and photoisomerization: Two competitive processes for merocyanine 540 irradiated with visible light. *J. Photoch. Photobio. B* **1**, 437–446.
29. Redmond, R. W. and J. N. Gamlin (1999) A compilation of singlet oxygen yields from biologically relevant molecules. *Photochem Photobiol.* **70**, 391–475.
30. Baptista M. S., J. Cadet, P. Di Mascio, A. A. Ghogare, A. Greer, M. R. Hamblin, C. Lorente, S. C. Nunez, M. S. Ribeiro, A. H. Thomas, M. Vignoni, T. M. Yoshimura (2017) Type I and Type II Photosensitized Oxidation Reactions: Guidelines and Mechanistic Pathways. *Photochemistry and Photobiology*. **93**(4), 912–919. http://dx.doi.org/10.1111/php.12716
31. Henderson, B. W. and T. J. Dougherty (1992) How does photodynamic therapy work? *Photochem. Photobiol.* **55**, 145–157.